The Behaviour of a Rod (Beam) Under the Influence of an External Power Load

Viktoriya Pasternak[1], Oleg Zabolotnyi[1](✉), Nataliia Ilchuk[1], José Machado[2], and Kostiantyn Svirzhevskyi[1]

[1] Lutsk National Technical University, 75, Lvivska Street, Lutsk 43018, Ukraine
volynasi@gmail.com

[2] Department of Mechanical Engineering, MEtRICs Research Centre, University of Minho, 4804-533 Guimarães, Portugal

Abstract. This paper justifies the primary conditions for the strength, rigidity, and stability of the part's structural elements (a mechanism). They presented the theoretical and practical part of the conditions for checking the strength of a beam (Rod). Graphically presented the stress σ_n, τ_n in height. We investigated the behavior of the rod (beam) model when calculating the tensile-compressive strength. Based on the results obtained, plots of longitudinal forces were constructed. It was found that at each point of the cross-section, internal bonds (forces-N) arise, which are evenly distributed. It should be noted that the constructed plots of tensile forces were carried out based on improved equilibrium equations. In this case, the axial force formed on the first section was determined by the algebraic sum of all forces located only on one side of the section. We investigated the strength conditions that did not exceed the limits of permissible limit norms. We also investigated the main parameters and limits of permissible norms of reference reactions, confirming a reliable test for all three main strength conditions. It should also be noted that the SolidWorks software product performed computer modeling based on strength analysis, which made it possible to design the main structural elements of this part. Also, to study the behavior of the calculated beam model under various influences in terms of static, part stability, natural frequency fluctuations, and external load application.

Keywords: Detail · Deformation · Reference reactions · Strength conditions · Cross-section · Statistical equations · Plots · Numerical analysis · Manufacturing innovation

1 Introduction

The study of real bodies is currently an urgent task since parts' behavior and model can deform (strain is a physical quantity, the result of a deforming load), changing their shape, position, and dimensions. Therefore, it is essential to consider the definition of all possible sizes of elements of any structure, in which the size of the part and their shape will not exceed the specified values, which are mainly determined by the

V. Ivanov et al. (Eds.): DSMIE 2022, LNME, pp. 13–22, 2022.
https://doi.org/10.1007/978-3-031-06044-1_2

operating conditions. It is also important to remember the stability of the structure itself and maintain the shape of the balance and size.

It should be noted that the deformation of bodies occurs due to the application of external force loads to them. When the body and its critical (dangerous) points, lines, or cross-sections are deformed, they move to another plane or space relative to their original (initial) position. Thus, one of the essential tasks of applied mechanics is to assess the strength and rigidity of any structure to ensure reliable and actual dimensions of the cross-section of the part.

2 Literature Review

After considering the scientific work presented in [1], it can be stated that the authors experimented with a general estimate of the flexural strength of the most significant productivity of the working areas of beams. At the same time, the research teams used such starting materials that contained small elements of fiber and alloy, which in turn caused destruction and cracks in the samples. In [2], the results of the reliability of the circular moment of a beam (rod) based on stress concentration coefficients and using the Monte Carlo modeling method are analyzed and justified. The authors of [3] focused their attention on the behavior of models of curved composite beams under constant load. At the same time, the limits of the maximum load, the maximum deviation, and the spread of a deep crack that occurred at the bends of the most dangerous points were not considered. In scientific studies presented in [4], standard conditions for the strength and shear of a part (beam) were considered.

It should be noted that the authors used outdated RC system designs. The scientific results covered in [5] are unusual. The authors pay special attention to the study of cross-sections and inclusions, which can improve the stress coefficient due to thermal expansion and the pyroelectric effect. Works [6] aim to experimental and analytical calculations of bending modernization of T-shaped beams using CFRP sheets. It is important to note that these structural materials do not fully provide the primary operating conditions. In [7], numerical intervention is based on strengthening steel beam profiles. Cold-formed steels that were used to make part profiles were subjected to various manufacturing scenarios and could bend. In this experiment, only a monotonous load was used. Research teams [8] investigated a fiber-based aggregate beam's width and crack propagation. The main goal was to reduce the spread of these cracks, as this is essential for protecting any reinforcement from various types of corrosion.

The authors of [9] investigated the technology and software tools for controlling samples made of structurally inhomogeneous materials. It should be noted that the proposed algorithm for recognizing problems of destruction (deformation) of samples is effective since it allows analyzing the surface and internal connections of materials, which makes it possible to improve the strength and stability of parts for any purpose. The efficiency of the DIC system for measuring beam reinforcement is highlighted in [10]. The authors investigated the strength-to-weight ratio of the part, its durability, and its low price. Linear differential results (LVDT) measurements were tested using a DIC system. Papers [11–13] performed numerical studies of the dynamic responses of various mechanical systems. Also, based on the obtained results, a model was developed

to simulate the study of the structural reaction of a T-shaped beam (rod) [14]. This simulation model functions only under shock load conditions. Works in [15] are based on the bending behavior of beams considered for stretching. It was found that high stress reduces the plasticity of the beam and violates the primary tensile condition [16]. In addition, samples made from hardened rebar have been shown to exhibit better limiting moments and ductility than samples made from hardened steel [17]. The main problems of vibration of beams (rod) are justified in the works [14]. The authors propose solving equations using linear variables and Coriolis force [18]. The article [19] is devoted to studying an S-shaped beam with uniform bending.

The extensive use of the ANSYS program with artificial neural networks is applied in [20, 21] for nonlinear analysis of the finite element beam method. In [22–24], new methods for strengthening are proposed. Polymer (CFRP) ropes were studied based on a T-shaped test cross-section that causes transverse displacement. Critical moments were recorded with the intervention of a monotonous load mode. The authors of this study claim that fatigue cracks strongly influence the manufacture of such structures and mechanisms. They propose to solve this problem using the methods of mathematical equations of Johnson and Cafoll. However, the literature review does not allow us to thoroughly study the behavior and model of parts under the influence of external force load. Thus, it is proposed to pay more attention to the cross-sectional dimensions of the rod (beam) based on improving the primary strength conditions.

3 Research Methodology

3.1 Primary Conditions for the Strength, Rigidity, and Stability of the Part

The article's primary purpose is to study reliable dimensions of the cross-section of a part (rod) using the SolidWorks software product, which is affected by external power loads.

It is necessary to perform calculations for the strength and rigidity of the beam to ensure the necessary stability of the elements of any structure or mechanism. To meet the strength conditions, the dimensions of the cross-section of the part (beam) must be determined from the conditions that the possibility of destruction is excluded under any action of an external force load. In turn, the destruction of the sample occurs due to the highest values of tangential stresses or normal stresses or the overlap of a simultaneous combination of them. Therefore, these values are limited to certain permissible values and are set by the following main parameters: σ is the normal stress; τ is the tangential stress.

It should also be noted that the following main elements of the study should be taken into account when calculating strength:

1. Design calculation (external loads acting on the material are known in advance, as a result of which it is necessary to find the dimensions of the cross-section of the part (rod)).
2. Verification calculation (structurally inhomogeneous material and part dimensions are known in advance. A mandatory condition for this calculation is to check the

conditions of the external power load and whether this structure or mechanism will withstand the external power load acting on it).
3. Correlation of the designed and tested calculations (previously known inhomogeneous material, part dimensions and its load scheme. The primary purpose of this calculation is to find out certain permissible values of normal and tangential stresses and what maximum external load the beam (rod) can withstand).

All the main elements (calculations) are based on certain strength conditions, which should not exceed the limit values: 100 mm^2–148 mm^2. Under which the effective value of the external force stress should not exceed the permissible values. That is, we get: $\sigma_{max} \leq \sigma$ and $\tau \leq \tau$.

It should be noted that the stiffness conditions were calculated based on the maximum values of linear and angular deformations. We obtain:

$$\Delta l \leq [\Delta l],\ \theta \leq [\theta] \tag{1}$$

where Δl – changing the part size; $[\Delta l]$ – acceptable values for this change; θ, $[\theta]$ – angular deformation, the angle of twisting of the structure (mechanism) and permissible values of this value.

3.2 Theoretical Part of Checking the Strength of a Beam (Rod)

Three main strength conditions must be met to implement and test the strength of a beam part:

1. the primary condition must correspond to the following ratio:

$$\sigma_{max} = \frac{M_{max}}{W_z} \leq \sigma \tag{2}$$

It should be noted that the check must be performed in the section where: $M(x) = M_{max}$.
2. $\tau = \frac{Q_{max} \cdot S_z}{d \cdot I_z} \leq \tau$. The condition must be met in the section where: $Q(x) = Q_{max}$.
3. $\sigma_r = \sqrt{\sigma_n^2 + 4\tau_n^2} \leq \sigma$. This check should be performed in the cross-section of the most problematic area of the part (beam), where: M(x) = Q(x) acts simultaneously. In this section of the most problematic zone, it is necessary to select a dangerous point of application of force F, which is simultaneously affected by normal and tangential stresses reaching large values σ_n, τ_n. In this case, the dangerous and problematic point of the part (beam) is the point "n", which is responsible for the transition from one element of the part to another. We get:

$$\sigma_n = \frac{M(x) \cdot y_n}{I_z} = \frac{M(x) \cdot \left(\frac{h}{2} - t\right)}{I_z}, \tau_n = \frac{Q(x) \cdot S^p}{d \cdot I_z} = \frac{Q(x) \cdot b \cdot t \cdot \left(\frac{h}{2} - \frac{t}{2}\right)}{d \cdot I_z}, \tag{3}$$

where: I_z – the moment of inertia relative to the axis z; S_z^p – the static moment of the axis area z.

Figure 1 shows plots of external stresses σ and τ, which are affected by large values of stresses σ_n, τ_n at the dangerous point «n» of the section.

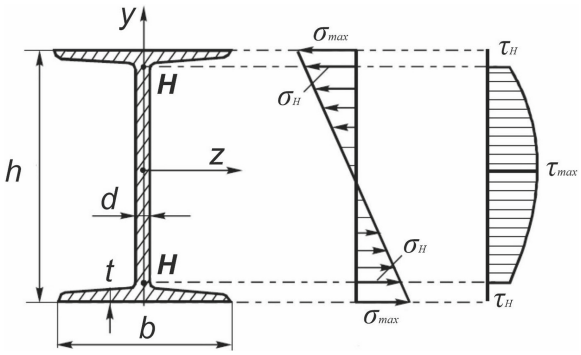

Fig. 1. Stress distribution σ_n, τ_n by height.

From this Fig. 1, it can be seen that the cross-section method determines the normal forces that occur in cross-sections. In this case, each section divides the beam (rod) into two parts. In this case, the actual direction of the normal force applied in relation to the cross-section is established when considering the equilibrium of one part of the part to another. To do this, it is necessary to consider the elementary equilibrium equation. If its weight is not considered when the part is stretched or compressed, then the normal forces must be determined using the specified external forces F_i. It was found that at each point of the cross-section, the internal bonds (forces) are evenly distributed. Thus, the internal forces per unit cross-sectional area are further determined by the normal stress σ.

4 Results

4.1 Model of Behaviour of the Rod (Beam) in the Calculation of Tension-Compression

It should be noted that any tensile-compressive calculation is based on the basic strength conditions that must comply with certain normative mathematical norms, we obtain:

$$\sigma_{max} \leq [\sigma], \quad \sigma_{max} = \frac{N_{max}}{A}, \quad \frac{N_{max}}{A} \leq [\sigma] \tag{4}$$

where N – longitudinal force; A – the cross-sectional area of the part (beam), measured in $\pi d^2/4$.

In this way, you can plot the longitudinal forces N in order to get the maximum value of N_{max}. Figure 2 shows the cross-sectional area in individual places where an external power load is applied. Where: $l = 600–700$ mm, $F = 11750$ [H], the material of the beam (rod) is steel, $[\sigma] = 158$ [H/mm^2].

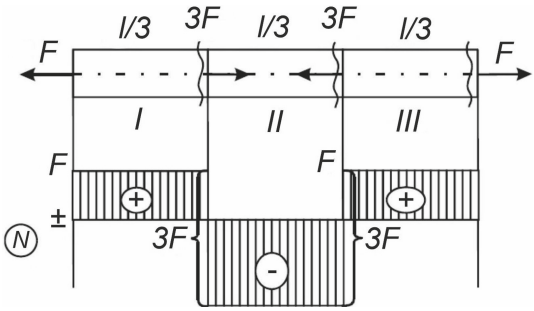

Fig. 2. The cross-sectional area of external power load application.

In Fig. 2, the formation of certain areas of cross-sections and end sections at the places where external forces are applied is visible. There is a selection of 3 sections I, II, III in this case. In turn, in the section in which a tensile or compressive external force is applied on plot N, we observe specific changes in fixed jumps by the amount of external force. So, in Fig. 3a) we present and consider plot I. And in Fig. 3b) section II is presented:

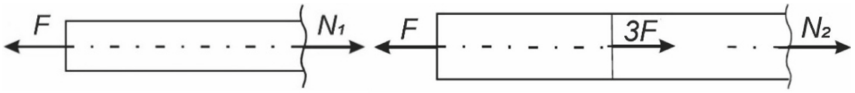

a) b)

Fig. 3. Plot area, where: a) plot area I; b) plot area II.

From the presented Fig. 3a) it can be seen that the equilibrium is equal to the following relation, we get: $\sum F_i = 0$. In this case, for the condition $F - N_1 = 0$, we use the following rule: the axial force formed on section I is determined by the algebraic sum of all forces located only on one side of the section. We found out that force F is tensile. Hence we got, $N_1 = F$. Thus, we obtained the following value of the force $N_1 = F$, which will be constant for the entire section (region) I.

After that, we considered the characteristic cross-section that occurs at the border of sections I and II (Fig. 3b)). It is worth noting that a compressive force of $3F$ acts in this section. According to the above rule, we conclude that the jump must be made to the negative zone by an amount of $3F$. That is, we get the following relation: $F - 3F = -2F$. After that, we consider the cross-section at the end of the selected area of Section II. we obtain the following equilibrium conditions:

$$\sum F_i = 0, F - 3F - N_2 = 0 \tag{5}$$

This leads to the following relation we get: $N_2 = F - 3F = -2F$. It should be noted that this is a constant value that acts on section II. It was found that the tensile force $3F$ acts in the cross-section of sections II and III. We get the following mathematical relation: $-2F + 3F = F$.

Considering the last section that occurs at the end of the region of section III, we can write the equilibrium equation on different sides of the section:

To the left $\rightarrow F - 3P + 3P - N_3 = 0$; It follows that $N_3 = F$.

To the right $\rightarrow F - N_3 = 0$; From here, we get: $N_3 = F$.

Accordingly, the strength conditions will take the following form:

$$\frac{2F}{A} \leq [\sigma] \tag{6}$$

From here, we get: $A = \frac{\pi d^2}{4} = \frac{2 \cdot 11750}{158} \geq 148{,}7\ \text{mm}^2$. It follows that $d \geq 1, 13\sqrt{A} \geq 13{,}7$ mm. Therefore, the more considerable value in the direction of the common value will be $d = 14$ mm.

4.2 Ensuring Beam Strength Based on Static Equations

To check the support reactions in certain sections *Q(x)* and *M(x)* of the beam (Fig. 4), it is necessary to perform a full-strength check of the part (point 3.2), as well as select the I-beam section.

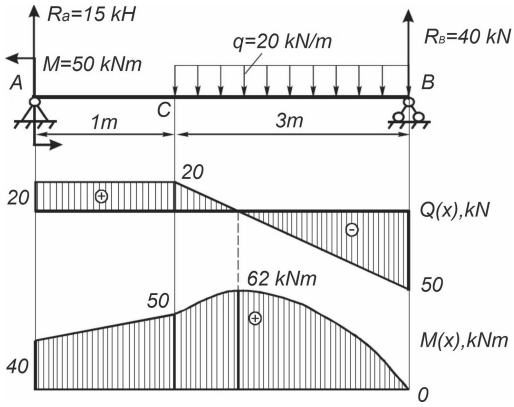

Fig. 4. General view of the beam (rod) diagram.

It should be noted that the normal and tangential stresses, in this case, are $\sigma = 170$ MPa, $\tau = 70$ MPa. In Fig. 4. the load diagram and transverse force plots are presented, as well as the bending moment of the beam is recorded. This study of the support reactions on certain sections of the beam (rod) showed that the plots *Q(x)* and *M(x)* are equal to the following parameters: $M_{max} = 62$ kNm, $Q_{max} = 40$ kNm. We found that the most dangerous cross-section is the section in zone *C*, where *M(x) = 50* kNm and *Q(x) = 20* kNm. The main parameters and limits of permissible norms of reference reactions, which were obtained based on the study (Fig. 4), are presented in Table 1.

Table 1. Basic parameters and limits of permissible norms of reference reactions.

Basic parameters	Limits of acceptable standards
R_A, kN	15
R_B, kN	40
W_Z, cm^3	406
I_Z, cm^4	5500
S_Z, cm^3	230
h, mm	260
b, mm	140
d, mm	7,0
t, mm	10,1

Therefore, we can conclude that a full test for all three main strength conditions is performed. Thus, this means that the strength of the selected part (beam) is fully ensured.

4.3 The Behavior of a Part (Beam) Using Computer Modelling

Computer simulations were performed in SolidWorks software. Since it was this functional modeling complex that allowed us to model a solid-state object by the finite element method. In Fig. 5, the model of the part–beam (rod) behavior is presented.

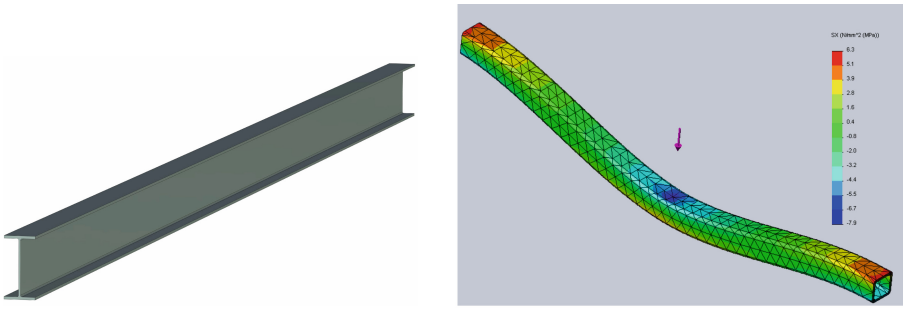

a) b)

Fig. 5. Part model using the SolidWorks software system, where: a) part model-beam (rod); b) generation of a finite element grid of the part-beam (rod).

As a result of the simulation performed by the SolidWorks system, we calculated the strength and rigidity of the part. Because of modeling, the following basic properties were set: thermal conductivity, density, Poisson's coefficient, yield strength; modulus of elasticity; coefficient of thermal expansion; tensile-compressive strength.

5 Conclusions

It was found that the maximum stress is ranged from 70 MPa to 170 MPa. It occurs at certain points in the cross-section, acts on the part, and distributed evenly. At the same time, all three main strength conditions are met, which lie within acceptable standards, which allows us to assert the reliability of the calculation results. Based on the calculations made, the following main factors were predicted: (1) load and voltage distribution; (2) occurrence of deformation in the part structure; (3) part stability margin coefficient, natural frequency fluctuations, and their shape; (4) preliminary temperature distribution in the part structure-beam (Rod); (5) this model's mass and moment of inertia relative to the x, y, and z coordinate system.

References

1. Chi-Young, J., Jong-Han, L.: Crack closure and flexural tensile capacity with SMA fibers randomly embedded on tensile side of mortar beams. Nanotechnol. Rev. **1**(9), 354–366 (2020)
2. Mayda, M.: Monte carlo simülasyon yöntemi ile dairesel delikli ankastre kirişin gerilme yiğilmasi faktörüne bağli güvenilirlik analizi. GU J. Sci. **6**(1), 241–249 (2018)
3. Abdulkhaliq, A., Saba, K.: Behavior of curved steel-concrete composite beams under monotonic load. Int. J. Math. Eng. Manag. Sci. **5**(6), 1210–1233 (2020)
4. Lavorato, D., Nuti, C., Santini, S.: Experimental ınvestigation of the shear strength of RC beams extracted from an old structure and strengthened by carbon FRP U-Strips. Appl. Sci. **8**(1182), 1–29 (2018)
5. Pasternak, Ia., Pasternak, R., Pasternak, V., Sulym, H.: Boundary element analysis of 3D cracks in anisotropic thermomagnetoelectroelastic solids. Eng. Anal. Bound. Elem. **74**, 70–78 (2017)
6. Yannian, Z., Moncef, N.: Experimental and analytical ınvestigation on flexural retrofitting of RC T-Section beams using CFRP sheets. Appl. Sci. **10**(1233), 1–14 (2020)
7. Taheri, Eh., Firouzianhaji, Ah., Mehrabi, P., Hosseini, B., Samali, B.: Experimental and numerical ınvestigation of a method for strengthening cold-formed steel profiles in bending. Appl. Sci. **10**(3855), 1–31 (2020)
8. Ghalehnovi, M., Karimipour, A., Brito, J., Reza Chaboki, H.: Crack width and propagation in recycled coarse aggregate concrete beams reinforced with steel fibres. Appl. Sci. **10**(7587), 1–27 (2020)
9. Zabolotnyi, O., Pasternak, V., Ilchuk, N., Huliieva, N., Cagáňová, D.: Powder technology and software tools for microstructure control of AlCu2 samples. In: Ivanov, V., Trojanowska, J., Pavlenko, I., Zajac, J., Peraković, D. (eds.) DSMIE 2021. LNME, pp. 585–593. Springer, Cham (2021). https://doi.org/10.1007/978-3-030-77719-7_58
10. Funari, M., Verre, S.: The effectiveness of the DIC as a measurement system in SRG shear strengthened reinforced concrete beams. Curr. Comput. Aided Drug Des. **11**(265), 1–11 (2021)
11. Ivanov, V., Pavlenko, I., Kuric, I., Kosov, M.: Mathematical modeling and numerical simulation of fixtures for fork-type parts manufacturing. In: Knapčíková, L., Balog, M. (eds.) Industry 4.0: Trends in Management of Intelligent Manufacturing Systems. EICC, pp. 133–142. Springer, Cham (2019). https://doi.org/10.1007/978-3-030-14011-3_12
12. Ivanov, V., Dehtiarov, I., Pavlenko, I., Kosov, M., Hatala, M.: Technological assurance and features of fork-type parts machining. In: Ivanov, V., et al. (eds.) DSMIE 2019. LNME, pp. 114–125. Springer, Cham (2020). https://doi.org/10.1007/978-3-030-22365-6_12

13. Huiling, Z., Xiangqing, K., Ying, F., Yihan, G., Xuezhi, W.: Numerical investigation on dynamic response of RC T-Beams strengthened with CFRP under impact loading. Curr. Comput. Aided Drug Des. **10**(890), 1–16 (2020)
14. Szewczak, I., Rozylo, P., Rzeszut, K.: Influence of mechanical properties of steel and CFRP tapes on the effectiveness of strengthening thin-walled beams. Materials **14**(2388), 1–14 (2021)
15. Elamary, Ah., Alharthi, Y., Abdalla, O., Alqurashi, M., Sharaky, I.A.: Failure mechanism of hybrid steel beams with trapezoidal corrugated-web non-welded ınclined folds. Materials **14**(1424), 1–18 (2021)
16. Barichello, C., Landesmann, Al., Camotim, D.: Distortional failure and DSM design of cold-formed steel S-shaped beams under uniform bending. Latin Am. J. Solids Struct. **14**(1), 2123–2140 (2017)
17. Chalioris, C., Kosmidou, P., Papadopoulos, N.: Investigation of a new strengthening technique for RC deep beams using carbon FRP ropes as transverse reinforcements. Fibers **6**(52), 1–18 (2018)
18. Wu, F., Tang, W., Xue, C., Sun, G., Feng, Y., Zhang, H.: Experimental investigation on the static performance of stud connectors in steel-HSFRC composite beams. Materials **14**(2744), 1–19 (2021)
19. Gencturk, B., Aryan, H., Hanifehzadeh, M., Chambreuil, C., Wei, J.: A computational study of the shear behavior of reinforced concrete beams affected from alkali–silica reactivity damage. Materials **14**(3346), 1–23 (2021)
20. Pavlenko, I., Simonovskiy, V., Ivanov, V., Zajac, J., Pitel, J.: Application of artificial neural network for identification of bearing stiffness characteristics in rotor dynamics analysis. In: Ivanov, V., et al. (eds.) DSMIE 2018. LNME, pp. 325–335. Springer, Cham (2019). https://doi.org/10.1007/978-3-319-93587-4_34
21. Basil, I., Moussa, L., Salah, A., Samer, B.: Shear strength of externally U-bonded carbon fiber-reinforced polymer high-strength reinforced concrete. Materials **14**(3659), 1–26 (2021)
22. Hurey, I., Gurey, V., Bartoszuk, M., Hurey, T.: Formation of residual stresses during discontinuous friction treatment. J. Eng. Sci. **8**(1), C38–C44 (2021). https://doi.org/10.21272/jes.2021.8(1).c5
23. Altoubat, S., Karzad, A., Maalej, M., Barakat, S., Junaid, T.: Experimental study of the steel/CFRP interaction in shearstrengthened RC beams incorporating macro-synthetic fibers. Structures **25**, 88–98 (2020)
24. Hovorun, T., et al.: Improvement of the physical and mechanical properties of the cutting tool by applying wear-resistant coatings based on Ti, Al, Si, and N. J. Eng. Sci. **8**(2), C13–C23 (2021). https://doi.org/10.21272/jes.2021.8(2).c3